

## MESOPOROUS SILICA-CALCIUM PHOSPHATE COMPOSITES FOR EXPERIMENTAL BONE SUBSTITUTION

István Lázár<sup>1</sup>, Sándor Manó<sup>2</sup>, Zoltán Jónás<sup>2</sup>, László Kiss<sup>2</sup>, István Fábíán<sup>1</sup>,  
Zoltán Csernátony<sup>2</sup>

<sup>1</sup> University of Debrecen, Department of Inorganic and Analytical Chemistry

<sup>2</sup> University of Debrecen, Department of Orthopaedic Surgery

[lazar@delfin.unideb.hu](mailto:lazar@delfin.unideb.hu)

### Introduction

Artificial materials of controlled strength, chemical composition and pore structure have gained significant attention in the medical practice in the last two decades. Synthetic materials used for bone substitution are of either inorganic or organic origin. Inorganic materials like tricalcium phosphate<sup>1,2</sup> and hydroxylapatite<sup>3</sup> are preferred nowadays, but other materials such as ceramics and bioceramics<sup>4</sup>, bioglass<sup>5,6</sup>, metals with bioactive ceramic surface coating<sup>7,8</sup> or calcium sulfate<sup>9,10</sup> are also in active duty. Organic substances, i.e. polylactic acid<sup>5</sup>, PMMA<sup>11</sup>, collagen or chitosan<sup>12,13</sup> are also widely used, most frequently in combination with one or more of the before-mentioned inorganic fillers.

Most recently the role of silica in living organisms has been revised and now is considered essential for the development of bone tissues<sup>14</sup>. Silica containing calcium phosphate have shown osteoinductivity in human osteoblast cultures in vitro<sup>15</sup> and preparations with various silica and calcium phosphate compositions are under clinical studies<sup>16</sup>.

Pore size distribution of bones and artificial bone substitute materials are of critical importance. Natural pores in the 100–1000  $\mu\text{m}$  region are required for bone tissue ingrowth, while smaller pores in the 10–100  $\mu\text{m}$  range conduct only the unmineralized fibrous tis-

sue<sup>17</sup> and contribute to materials transport. Most recently ordered structure silicas like MCM-41 are under investigation in combination with polylactic acid or other biopolymers as new, high porosity bone substitutes<sup>5</sup>.

Sol-gel technology opened the way to the synthesis of mesoporous silicas that can be used as extremely high porosity matrix and excellent drug delivery materials. In combination with calcium ions containing inorganic materials they may represent the third generation of bone substituent bioceramics<sup>18</sup>. Based upon our earlier experiences in aerogel synthesis and supercritical drying technology we have decided to synthesize potentially bioresorbable composite materials containing calcium phosphate powder and mesoporous silica of controlled pore size.

### Methods

#### Materials

Tetramethoxysilane (TMOS, 98%) was purchased from Fluka, microgranular cellulose from Sigma, methanol (purum), acetone (purum) and ammonia solution (analytical grade, 25%) from Acidum-2 Kft. (Debrecen, Hungary), tricalcium phosphate (Ph Eur) from a local pharmacy. Triple deionized, membrane and carbon filtered water was prepared with a water station, which was constructed of a high capacity double ion exchange battery con-

nected to a high purity MilliQ instrument. Carbon dioxide cylinders were purchased from Linde.

#### **Methods and instrumentation**

Plastic molds (approx. 70 mm tall) were machined from a regular pvc waterwork pipe of 28/32 mm id/od. The inner walls of the molds were covered with thin teflon foil. The bottom of the molds were sealed with multiple layers of parafilm. Supercritical carbon dioxide drying was performed in a custom made 1.5 L volume stainless steel SCO<sub>2</sub> dryer at 70–80 °C. Heating and sintering of the samples was carried out in a 14 L volume WiseTherm rectangular furnace, the temperature accuracy was better than  $-1/+3$  °C at 1150 °C.

Compressive stress of the samples were determined with a INSTRON 8874 Servohydraulic Biaxial Material Testing Machine. Thermogravimetric and thermoanalytical measurement was carried out with a MOM Derivatograph-C instrument in the 100–1200 °C range. Scanning electron microscopic images were recorded on a Hitachi S-4300 CFE instrument.

#### **Cellulose-tricalcium phosphate alcogel**

To a vigorously stirred solution of 21.00 mL (21.48 g, 0.1411 mol) of tetramethoxy silane (TMOS), 154 mL (121 g, 3.80 mol) of methanol (MeOH), 14,0 mL (14.0 g, 0.77 mol) of water was added 7.00 g of microgranular cellulose and 7.00 g of very finely powdered tricalcium phosphate. The mixture was sonicated in a common laboratory ultrasonic bath for 1–2 minutes to evenly disperse the solids, then stirred vigorously meanwhile 35 mL of ammonium hydroxide (25 m/m%, 0.47 mol NH<sub>3</sub>) was added in one portion. The homogenous mixture was poured rapidly into the plastic molds, sealed and let to stand at room temperature for several days. Setting occurred within a few ten seconds to a few minutes,

depending on the actual temperature and the length of ultrasound treatment. The longer was the sonication, the shorter was the setting time. (Note that changing of the molar ratios or particle size of the solid components may lead to too short or too long setting times or to sedimentation of tricalcium phosphate. Some experimentation might be necessary to find the optimal conditions.)

#### **Preparation of X1-700 and X1-900 xerogels**

Cellulose-tricalcium phosphate alcogel monoliths were pushed out of the molds with a machined plunger and placed into a Petri dish lined with five layers of round filter paper. To avoid cracking and ensure uniform drying the monoliths were surrounded and covered nearly airtight with cylinders made of several layers of regular filter paper and let to stand and dry under a hood for several days. In this period significant linear shrinking occurred, but cracks did not appear. The resulted gels were dried in an oven at 100–110 °C for at least one day, then heated in a furnace at 700 °C for 5 hours to burn out cellulose and reach the final structure and dimensions (shrinking from 28.0 mm od. to 14.5 mm od. occurred). Those xerogels were still fairly fragile and sensitive pieces, which could be broken easily by bare hands (Sample X1-700).

A X1-700 xerogel monolith was sintered at 900 °C for 12–24 hours to reach the required mechanical strength. It shrunked further to a final diameter of 10.5 mm, and its strength increased so much that it could not be broken by bare hands any more (Sample X1-900).

#### **Preparation of A1-SC aerogel**

Water and alcohol content of the alcogel monoliths were replaced with acetone in the following manner. The alcogels were pushed out of the plastic molds and soaked first in pure methanol, then in methanol-acetone mixtures (acetone content was increased gradually

in 25% steps) and in acetone, for one day in each solvent mixtures. Acetone gels were then transferred into the  $\text{SCO}_2$  dryer under acetone. After sealing the reactor body, acetone was drained and flushed with liquid carbon dioxide. Remaining acetone entrapped in the gel bodies was expelled by liquid carbon dioxide and formed an immiscible secondary liquid phase in the bottom of the reactor. This was drained in several portions in a 4–12 hours period of time. The system was considered acetone-free when dry ice collected from the flushing carbon dioxide gave no liquid residue evaporated on a horizontal steel surface. The temperature was then increased to and kept at approximately 60–70 °C for at least one hour, then the pressure was released in 3–4 hours through a needle valve and a capillary made of a 100 mm long 1/16" od. 0.005" id. HPLC steel tubing. The aerogel samples were removed from the reactor and stored either in a heated cabinet at 110 °C or in sealed vials (Sample A1-SC).

#### Preparation of A1-1000 aerogel

Aerogel sample A1-SC was sintered in a furnace at 1000 °C for 6 hours resulting in a significantly shrunk aerogel monolith.

#### Tricalcium phosphate alcogel

To a vigorously stirred solution of 12.60 mL (12.89 g, 0.085 mol) of TMOS, 92 mL (73 g, 2.27 mol) of MeOH, 8.4 mL (8.4 g, 0.47 mol) of water was added 7.00 g of very finely powdered tricalcium phosphate. The mixture was sonicated for a short while to evenly disperse the solids, then stirred very vigorously meanwhile 21 mL of ammonium hydroxide (25 m/m%, 0.28 mol  $\text{NH}_3$ ) was added in one portion. The homogenous mixture was vigorously stirred until the viscosity had increased significantly, then poured rapidly into plastic molds. Bamboo sticks (soaked in methanol before, dimensions: 3 mm×3 mm×70 mm) were inserted into one of the monoliths before set-

ting occurred to make a hexagonally ordered template. The molds were then sealed and let to age at room temperature for several days. (Note that it is quite difficult to catch the right moment for casting to prevent rapid sedimentation of tricalcium phosphate granules, therefore preliminary experimentation is recommended. Moderate increase or decrease of the volume of ammonium hydroxide may also be necessary, as the concentration depends on the brand, the temperature and the age of the solution.)

#### Preparation of tricalcium-phosphate aerogels A2-SC

These samples were prepared by the same supercritical drying method as given for A1-SC aerogel. From the templated aerogel the bamboo sticks could have been pulled out without cracking of the monolith and left rectangular channels behind.

#### Preparation of A2-1000 aerogel

A2-SC aerogel samples were sintered at 1000 °C for 6 hours in a furnace.

### Results and discussion

#### Effect of drying technique on gel structures

The alcogel samples were dried by two different ways. The first one was ambient drying at room temperature, followed by heating in a furnace, which gave higher density, significantly shrunk xerogels X1-700 and X1-900. The second one was supercritical carbon dioxide drying resulted in aerogel samples A1-SC and A2-SC, from which samples A1-1000 and A2-1000 were prepared by heating at 1000 °C. Xerogels showed increased pore sizes and loss of mesoporosity compared to the corresponding aerogel analogs, which was the consequence of shrinking and deterioration of the aerogel structure due to the presence of capillary forces in the atmospheric drying phase.

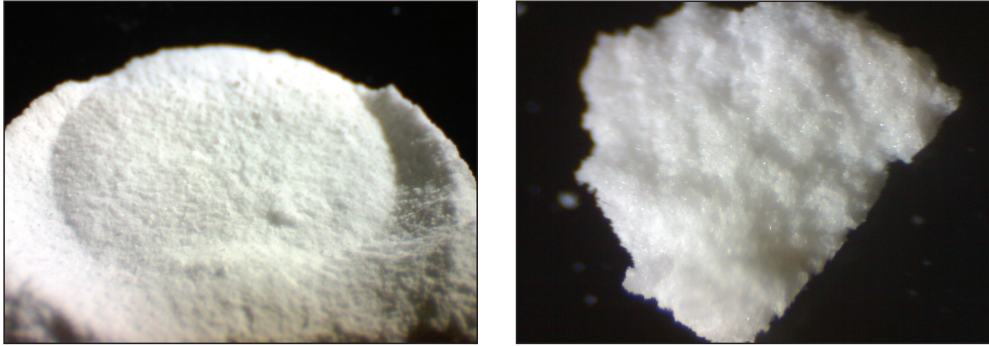


Figure 1. Optical microscopy images of silica-tricalcium phosphate xerogel monolith X1-900 in 16 $\times$  and 120 $\times$  magnification, respectively

Figure 1 shows optical microscopic picture of the X1-900 monolith. The grainy structure proved to be characteristic to all calcium-phosphate powder containing silica composites.

#### Structure of aerogel composites

Chemical composition of the aerogel and xerogel samples were identical for all of the samples as follows (calculated, expressed as oxides): SiO<sub>2</sub> 54.3 %, CaO 24.8 %, P<sub>2</sub>O<sub>5</sub> 20.9%. Cellulose was used as a disposable template material for the creation of pores in the submicron and microne range and can be burned out at 500 °C. Figure 2 shows the SEM pictures of A1-1000 and A2-1000 aerogels. It can be seen quite well that burnt cellulose left

large pores behind in the matrix, the pore diameters are in the range of approx. 100–7000  $\mu\text{m}$ , which belongs to the macropore region. A2-1000 shows a normal aerogel structure characterized by evenly distributed mesopores in the 10–100  $\mu\text{m}$  range.

Optical microscopic images show the difference between the macrostructures of A1-SC and A2-SC aerogel composites in Figure 3. In sample A1-SC the optical transparency is much lower and the gel structure seems to be more homogeneous than in A2-SC. The difference is most likely due to the presence of cellulose in A1 aerogel in the setting phase. Cellulose and calcium phosphate together

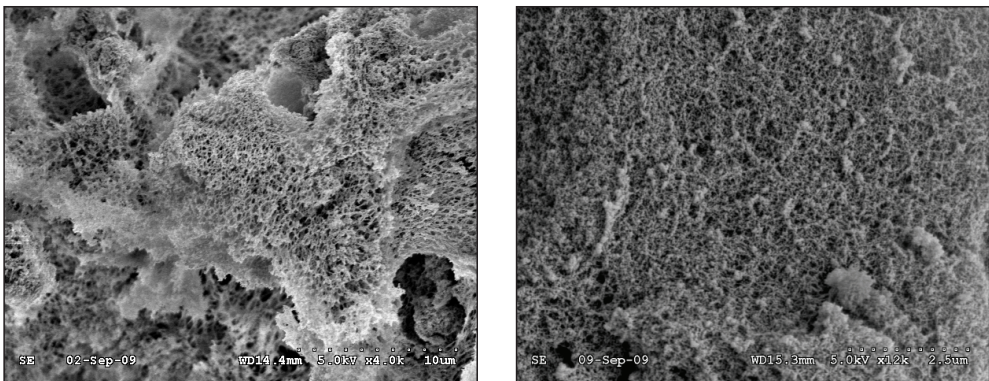


Figure 2. SEM pictures of composite aerogel samples A1-1000 and A2-1000. Magnification of the left and right pictures are 4k and 12k, respectively

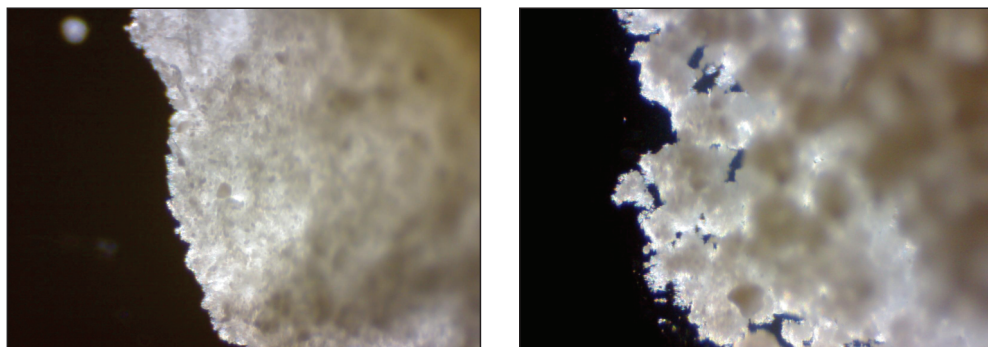


Figure 3. Microscopic images of aerogels A1-SC (left) and A2-SC (right) in 120 $\times$  magnification. Aerogel matrix is transparent and almost completely invisible in the right picture (some blueish tint can be observed between the seeds)

provided a much higher number of seeds for crystal forming, while in the A2 alcojel the relatively large particles of tricalcium phosphate were present in much less number resulting in formation of large condensed particles, which were embedded in and connected by a nearly transparent silica aerogel matrix.

### Sintering, shrinking

Changes of density and length of the aerogel sample A1-SC on heating was studied and the results are represented in Figure 4. The sample was heated for 24 hours at each temperature given, except for 1000  $^{\circ}\text{C}$  and 1050  $^{\circ}\text{C}$ , which were kept for 3 and 1 hours, respectively. As

it can be seen in Figure 4 the linear shrinking was moderate until 700  $^{\circ}\text{C}$  (1073 K) and became very significant above 800  $^{\circ}\text{C}$ . The virtual density of the sample decreased a bit at low temperature due to desorption of adsorbed solvents and water, then remained nearly unchanged (0,09  $\text{g}/\text{cm}^3$ ) between 500  $^{\circ}\text{C}$  and 600  $^{\circ}\text{C}$  and then increased significantly over 800  $^{\circ}\text{C}$  to reach 0.49  $\text{g}/\text{cm}^3$  value at 1000  $^{\circ}\text{C}$ .

Extended heating of the sample at 12 h/ 1000  $^{\circ}\text{C}$  and then 3h/1050  $^{\circ}\text{C}$  resulted in even higher densities of 0.75  $\text{g}/\text{cm}^3$  and 1.04  $\text{g}/\text{cm}^3$ , respectively. The sample shrank to 38% of the original length by reaching 1050  $^{\circ}\text{C}$ .

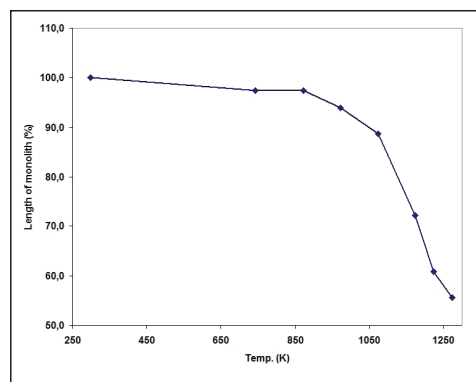
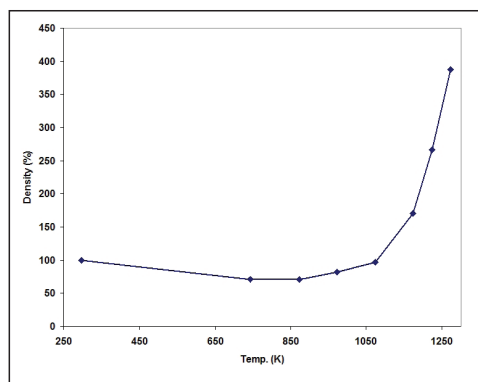
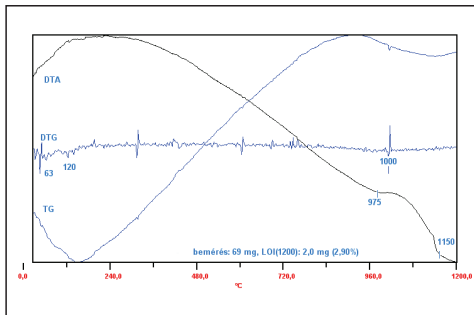


Figure 4. Change of relative density and length of aerogel monolith A1-SC versus the sintering temperature

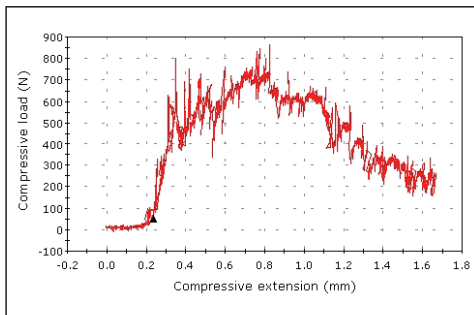
### Thermogravimetry analysis

Thermic behaviour of sample A1-700 was studied by thermogravimetry/differential thermoanalysis technique. 69 mg amount of aerogel was tested and the change of weight and inner temperature was recorded as a function of time. TG-DTG-DTA curves of sample A1-700 can be seen in *Figure 5*.

At the first part of the DTA curve an endothermic change can be observed, which is in accordance with the loss of weight in the TG curve. Both end by approx. 240 °C and the phenomenon corresponds to the desorption of water. From 240 °C to 975 °C no thermic process occurred in the gel. At 975 °C an exothermic coalescence of the fine silica matrix has started and finished by 1150 °C. This process can be attributed in minor part to the condensation of silanol groups and in major part to the reduction of surface (by melting and



*Figure 5.* TG-DTG-DTA curves of sample A1-700



slow viscous flow) in the aerogel and led to the formation of large grains in the micron range.

### Mechanical testing

Cylindrical specimens of X1-900 and A2-1000 with known geometry were placed in the servohydraulic tester between 2 mm thick hard polypropylene plates. Compressive load vs. compressive extension curves (*Figure 6*) were recorded by using the 10 kN probe and compressive stress values were calculated. Compressive stress of aerogel sample A1-900 has also been determined, but its value was very low (0.28 MPa). This weakening of the aerogel composite structure was most likely the consequence of the presence of large pores and thin walls that were formed on baking out cellulose from the gel.

The calculated compressive stress values of X1-900 and A2-1000 samples were 18.2 MPa and 35.1 MPa, respectively. These values can be considered fairly promising in the point of view of potential bone substitution, as they reached or exceeded the average strength of natural cancellous bones.

### Conclusions

Two drying techniques have been developed for the preparation of tricalcium phosphate containing high porosity materials based

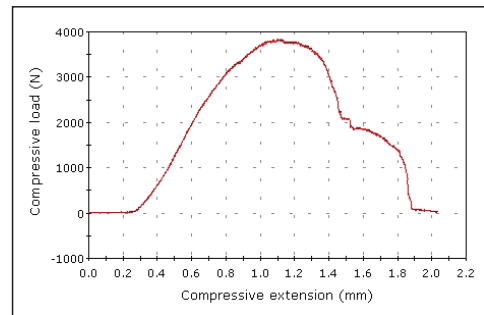


*Figure 6.* Compressive load vs. compressive extension curves of X1-900 (left) and A2-1000 (right) samples

on silica aerogels or xerogels for artificial bone substitution. Xerogel sample X1-900 was more simple to make by ambient drying but showed somewhat less mechanical strength. Silica aerogel A2-1000, which contained evenly distributed tricalcium phosphate particles embedded and chemically bonded in silica aerogel showed the highest compressive strength and reached the strength of cancellous bones. Based upon our experimental data, this tri-

calcium phosphate-silica aerogel composite prepared by the sol-gel technology and supercritical drying have the potential to be used as an artificial bone substitute. In addition, the characteristic aerogel pore structure offers an extra possibility to be used not just as bone substitute but also as a slow release drug carrier, which might be used for simultaneous treatment of bone infections or other diseases.

## REFERENCES

1. *Kamitakahara M, Ohtsuki C, Oishi M, Ogata S, Miyazaki T, Tanihara M.* Preparation of porous biphasic tricalcium phosphate and its in vivo behavior. *Key Engineering Materials* 2005;284–286, 281–284.
2. *Li P, Zhang K, Colwell CW Jr.* Experimental Study on the Osteoinduction of Calcium Phosphate Biomaterials In Vivo and the Capability of Supporting Osteoblast Proliferation In Vitro. *Key Engineering Materials* 2005;284–286, 293–296.
3. *Gerber T.* Production of highly porous ceramics for artificial bone. DE 19825419, 19991209, 1999.
4. *Chevalier J, Gremillard L.* Ceramics for medical applications: A picture for the next 20 years. *Journal of the European Ceramic Society* 2009;29: 1245–1255.
5. *Korventausta J, Rosling A, Andersson J, Lind A, Linden M, Jokinen M, Yli-Urpo A.* Bioactive glass (S53P4) and mesoporous MCM-41-type SiO<sub>2</sub> adjusting in vitro bioactivity of porous PDLA. *Key Engineering Materials* 2004;254–256, 557–560.
6. *Ohtsuki C, Kamitakahara M, Miyazaki T.* Bioactive ceramic-based materials with designed reactivity for bone tissue regeneration. *Journal of the Royal Society Interface* 2009;6:S349–S360.
7. *Liu X, Morra M, Carpi A, Li B.* Bioactive calcium silicate ceramics and coatings. *Biomedicine & Pharmacotherapy* 2008;62:526–529.
8. *Meretoja VV, De Ruijter AE, Peltola TO, Jansen JA, Naerhi TO.* Osteoblast Differentiation with Titania and Titania-Silica-Coated Titanium Fiber Meshes. *Tissue Engineering* 2005;11:1489–1497.
9. *Gisep A, Rahn B.* Calcium-Phosphate – Calcium-Sulphate Bone Cements. Structure and Compression Strength after Setting. *European Cells and Materials* 2004;7(Suppl. 2):34–35.
10. *Guo H, Wei J, Liu CS.* Development of a degradable cement of calcium phosphate and calcium sulfate composite for bone reconstruction. *Biomedical Materials* 2006;1:193–197.
11. *Shinzato S, Kobayashi M, Mousa WF, Kamimura M, Neo M, Kitamura Y, Kokubo T, Nakamura T.* Bioactive polymethyl methacrylate-based bone cement: comparison of glass beads, apatite- and wollastonite containing glass-ceramic, and hydroxyapatite fillers on mechanical and biological properties. *Journal of Biomedical Materials Research* 2000;51:258–272.
12. *Lee E-J, Shin D-S, Kim H-E, Kim H-W, Koh Y-H, Jang J-H.* Membrane of hybrid chitosan-silica xerogel for guided bone regeneration. *Biomaterials* 2009;30(5):743–750.

13. *Muzzarelli RAA*. Chitins and chitosans for the repair of wounded skin, nerve, cartilage and bone. *Carbohydrate Polymers* 2009;76:167–182.
14. *Martin KR*. The chemistry of silica and its potential health benefits. *Journal of Nutrition, Health & Aging* 2007;11(2):94–98.
15. *Phan PV, Grzanna M, Chu J, Polotsky A, El-ghannam A, Van Heerden D, Hungerford DS, Frondoza CG*. The effect of silica-containing calcium-phosphate particles on human osteoblasts in vitro. *Journal of Biomedical Materials Research, Part A* 2003;67A(3):1001–1008.
16. *Bienengraeber V, Gerber T, Trykova T, Kundt G, Henkel K-O*. A new high porous silica-sol-gel-ceramics for bone grafting – in-vivo long-time investigations. *Materialwissenschaft und Werkstofftechnik* 2004;35(4):234–239.
17. *Karageorgiou V, Kaplan D*. Porosity of 3D bio-material scaffolds and osteogenesis. *Biomaterials* 2005;26:5474–5491.
18. *Izquierdo-Barba I, Colilla M, Vallet-Regi M*. Nanostructured Mesoporous Silicas for Bone Tissue Regeneration. *Journal of Nanomaterials* 2008, 2008, Article ID 106970.

*Financial support from the Hungarian Research Fund (OTKA 76834) is gratefully acknowledged. The authors would like to express their thank to Lajos Daróczy (Department of Solid State Physics) and István Papp (Department of Mineralogy and Geology) for their kind help in electron microscopy and thermogravimetric examinations.*

**István Lázár**

University of Debrecen, Department of Inorganic and Analytical Chemistry  
H-4032 Debrecen, Egyetem tér 1.